Abnormal 8 Hz flicker electroretinograms in carriers of X-linked retinoschisis.

J. Jason McAnany[a,b,c*]

Jason C. Park[a]

Frederick T. Collison[d]

Gerald A. Fishman[a,d]

Edwin M. Stone[e]

[a]Department of Ophthalmology and Visual Sciences, University of Illinois at Chicago, 1855 W. Taylor St., Chicago, IL 60612, USA

[b]Department of Psychology, University of Illinois at Chicago, 1007 W. Harrison St., Chicago, IL 60612, USA

[c]Department of Bioengineering, University of Illinois at Chicago, 851 South Morgan St., Chicago, IL 60607 USA

[d]The Pangere Center for Hereditary Retinal Diseases, The Chicago Lighthouse for People Who Are Blind or Visually Impaired, Chicago, IL, USA

[e]Stephen A. Wynn Institute for Vision Research, Department Ophthalmology and Visual Sciences, The University of Iowa, Iowa City, IA, USA

[*]Corresponding author: J. Jason McAnany

Tel.: +1-312-355-3632.
e-mail address: jmcana1@uic.edu

Acknowledgments

This research was supported by National Institutes of Health Research Grants R00EY019510 (JM), P30EY001792 (UIC core grant), an unrestricted departmental grant from Research to Prevent Blindness, the Pangere Family Foundation, and the Grousbeck Family Foundation (GAF and EMS).

Abstract

Purpose: To evaluate rod-isolated, cone-isolated, and combined rod and cone flicker electroretinograms (ERGs) as a possible means to identify electrophysiological abnormalities in carriers of X-linked retinoschisis (XLRS). **Methods:** Full-field ERGs were recorded from 6 carriers of XLRS (ages 34 to 66 years) and 8 normally-sighted subjects (ages 27 to 59 years) under rod-isolated (ERG_R), cone-isolated (ERG_C), and combined rod and cone (ERG_{R+C}) conditions. ERGs were obtained using a 4-primary LED-based ganzfeld photostimulator and standard recording techniques. The 4 primaries were modulated sinusoidally in phase to achieve combined rod and cone activation (ERG_{R+C}) or in different phases to achieve ERG_R and ERG_C by means of triple silent substitution. After 30 minutes of dark adaptation, 8 and 15 Hz ERG_R, ERG_C, and ERG_{R+C} responses were obtained at a mean luminance level of 24 scot. cd/m^2. Standard ISCEV ERGs were also obtained from each subject. **Results:** The ISCEV and 15-Hz flicker ERGs were generally within the normal range for the carriers. The 8-Hz ERG_R, ERG_C, and ERG_{R+C} amplitudes were also generally normal. In contrast, the carriers had ERG_R, ERG_C, and ERG_{R+C} timing abnormalities, with phase advances beyond the range of normal for the ERG_R (4 carriers), ERG_C (4 carriers), and ERG_{R+C} (3 carriers). Only one carrier had normal 8-Hz responses under all conditions.

Conclusions: The 8-Hz ERG timing abnormalities in 5 of 6 carriers indicate that retinal function is not necessarily normal in carriers of XLRS. The 8-Hz flicker ERG may be useful for studying retinal function in these individuals.

Keywords: electroretinogram (ERG); rod; cone; flicker; X-linked retinoschisis

Introduction

Mutations in the retinoschisin gene (*RS1*) cause juvenile X-linked retinoschisis (XLRS) [1,2]. This hereditary, vitreoretinal degenerative disease is typically characterized by cystic-appearing foveal lesions and visual acuity loss in the first or second decade of life in affected males [3-6]. Approximately 50% of patients also develop peripheral retinoschisis [6]. The dark adapted full-field electroretinogram (ERG) can be useful in the diagnosis of XLRS because it shows a selective, or predominant, loss of b-wave amplitude [7]. In addition to the well-known b-wave loss under scotopic conditions, patients with XLRS can also have cone-pathway abnormalities. For example, some [8-10] but not all [8,9,11] patients have abnormal 30-Hz flicker ERGs, characterized by reduced peak-to-trough amplitude. The flicker ERG has also been recorded in these patients at frequencies that are lower and higher than the International Society for Clinical Electrophysiology of Vision (ISCEV) standard 30 Hz flicker frequency [8]. Interestingly, at low temporal frequencies (e.g. 8 Hz), patients with XLRS tend to have super-normal amplitudes and phase advances, whereas at high temporal frequencies (e.g. 64 to 100 Hz), patients can have marked amplitude losses and phase delays [8]. This pattern of temporal frequency deficit has been attributed to an abnormality in ON pathway function, which is consistent with their selective b-wave attenuation [8,12].

Although visual function in patients with XLRS has been well-studied, there are relatively few reports of visual function in carriers of XLRS. This is likely to be because female carriers of XLRS are typically assumed to have normal fundus features, visual acuity, and standard ISCEV ERGs [3,4,13]. However, a few reports have documented

subtle retinal changes, such as a wrinkling of the internal limiting membrane [14], and patchy losses of multi-focal ERG amplitude in some carriers [15]. Additionally, in a sample of 11 obligate carriers of XLRS, psychophysically measured cone flicker thresholds were found to be abnormal in each carrier, which was attributed to altered rod-cone interactions [16]. The generally normal findings based on standard clinical tests in carriers of XLRS differ from other X-linked retinal diseases, such as X-linked retinitis pigmentosa, choroideremia, and X-linked ocular albinism, in which female carriers can express some features of the disease. The abnormalities in these carriers can be explained on the basis of Lyonization, which predicts a random inactivation of one X chromosome in each cell [17-19]. The explanation for why carriers of XLRS apparently do not express features of the disease is unclear.

The purpose of the present study was to evaluate rod-isolated, cone-isolated, and combined rod and cone flicker ERGs as a possible means to identify functional abnormalities in carriers of XLRS. ERGs elicited by three types of temporally modulated stimuli were recorded: 1) rod-isolating stimuli in which cone excitation was kept constant (ERG_R), 2) cone-isolating stimuli in which S-, M-, and L-cone excitations were modulated in phase while keeping the rod excitation constant (ERG_C), 3) combined rod and cone modulating stimuli in which both rod and cone excitations were modulated in phase (ERG_{R+C}). This latter condition is of particular interest because it permits examination of rod-cone interactions in the ERG [20], for which abnormalities may be expected based on the previously reported abnormal psychophysical rod-cone interactions [16]. Our focus was on low frequency flicker (8 and 15 Hz) because of the flicker ERG abnormalities reported at these frequencies in patients with XLRS [8,12]

and because responses to the ISCEV standard 30 Hz flicker are generally thought to be normal in carriers of XLRS [13].

Methods

Subjects

Six female presumed carriers of XLRS (ages 34 to 66 years; Table 1) participated in this study. Five of the six carriers have a son with a molecularly proven mutation in the *RS1* gene (Table 1). Carrier 1 does not have children, but her father and a male first cousin both have a clinical diagnosis of XLRS based on classic fundus features including a spoke-wheel pattern of macular schisis and functional abnormalities including visual acuity loss and a reduced ERG b/a amplitude ratio (her family members have not been genotyped). Four of the 6 carriers (No. 1, 2, 4, 6) were “obligate carriers” based on a pedigree that showed either an affected father, brother, or another son (in addition to the proband); in the other two families, only the proband was affected.

Dilated fundus examination was unremarkable for all carriers. Additionally, the carriers all had ETDRS best-corrected visual acuity of 0 log MAR or better (equivalent to 20/20 or better Snellen acuity), no clinically significant ocular media opacities, no history of significant ocular abnormalities, and spherical refractive error less than 6.0 diopters. Each carrier underwent light and dark adapted ERG testing according to ISCEV standards [21].

Eight visually-normal control subjects (4 male and 4 female; ages 27 to 59 years) with no history of eye disease, normal color vision (Oculus Heidelberg Multi-Color Anomaloscope), and ETDRS best-corrected visual acuity of 0 log MAR or better also participated in the study. An independent samples t-test indicated that the mean age of

the controls (42.3 years) did not differ significantly from that of the carriers (53.7 years; $t = 2.08$, $p > 0.05$). Informed consent was obtained from all subjects before their participation. Procedures adhered to the tenets of the Declaration of Helsinki, and the protocol was approved by an Institutional Review Board at the University of Illinois at Chicago.

Apparatus and Stimuli

The apparatus and stimuli are described in detail elsewhere [22,23]. In brief, full-field stimuli were generated by a Diagnosys Espion E^3 system and presented in a ColorDome desktop ganzfeld (Diagnosys LLC, Lowell, MA). The LEDs of the ColorDome were programmed to serve as a four-primary photostimulator with dominant wavelengths of 465 nm (blue), 515 nm (green), 593 nm (amber), and 642 nm (red). The four LEDs were simultaneously modulated sinusoidally in phase to achieve combined rod and cone modulation or in different phases to achieve rod or cone isolation, as defined elsewhere [23,24]. A constant chromaticity was maintained under all three paradigms (CIE 10^o coordinates of $x = 0.58$ and $y = 0.40$). ERGs were recorded at a mean luminance level of 24 scot. cd/m^2 (33 phot. cd/m^2) at stimulus temporal frequencies of 8 and 15 Hz. Stimulus wavelength and luminance were measured using a Spectrascan 740 spectroradiometer (Photo Research, Chatsworth, CA). The Michelson contrast of the rod- and cone-isolating stimuli was 40%, which is the maximum achievable contrast under the cone-isolating paradigm. For the combined rod and cone stimulus, the rods and cones were modulated simultaneously in phase, each at 40% Michelson contrast. The mean luminance (scotopic and photopic cd/m^2), Michelson contrast, and relative phase of each LED are provided in Table 2.

As discussed elsewhere [23,24], the degree of rod and cone isolation is a potential concern in silent substitution paradigms, like that used in the present study. However, a recent study from our group [23] that used identical 15-Hz rod-isolating, cone-isolating, and combined rod and cone modulating stimuli and instrumentation found good isolation, based on results obtained from a patient who lacked a cone response (i.e. a complete achromat). Further evidence for our ability to achieve appropriate isolation is presented in the Discussion.

Procedure and ERG recording

Prior to the ERG recordings, the pupil of the tested eye was dilated with 1% tropicamide and 2.5% phenylephrine hydrochloride drops and the subject was dark-adapted for 30 min. ERGs were recorded with DTL plus fiber electrodes; ear clip and gold cup (forehead) electrodes served as reference and ground, respectively. Responses were acquired with an Espion E^3 electrophysiology console, with amplifier bandpass settings of 0.30–500 Hz at a sampling frequency of 1 kHz.

For each temporal frequency, 5 to 10 ERG sweeps were recorded. Each sweep was approximately 5 sec in duration (the exact duration of the sweep depended on the stimulus period), with an even number of cycles. The stimulus modulation was followed by a dark interval (minimum of 7 seconds) before the next sweep began.

Data Analysis

The initial 8 or 16 cycles, for the 8 and 15 Hz frequencies, respectively, were omitted from the analysis to avoid onset transients (approximately 1 sec). The remaining 32 or 60 cycles for the 8 and 15 Hz frequencies, respectively (approximately 4 sec), of each sweep were divided into an even number of segments and these

segments were averaged. This procedure was repeated for each of the 5 to 10 sweeps to generate an overall average for each subject. Fast Fourier transforms (FFTs) were performed on the overall average to derive the amplitude and phase of the fundamental component. In the figures below, the phases are given in cosine phase and are "unwrapped" to extend beyond 360°, per convention. A subject's response at a given stimulus frequency was considered distinguishable from noise if the amplitude at the stimulus frequency (8 or 15 Hz) was at least 2.82-times larger than the mean of the noise amplitudes measured at neighboring frequencies (±1 Hz above and below the stimulus frequency). As discussed elsewhere [25], this signal-to-noise ratio (SNR) corresponds to a significance level of $p = 0.05$. Individual responses that did not achieve an SNR of at least 2.82 were excluded from the results presented below.

Results

The amplitudes and implicit times of the ISCEV standard responses are provided in Table 3. The ERG amplitude and timing were generally within the limits of normal for the carriers, with the exception of Carrier 1, who had slightly reduced a-wave amplitude and substantially reduced b-wave amplitude recorded under the dark-adapted 3.0 cd s m^2 condition. Her b/a wave ratio was smaller than normal, a finding commonly observed in patients with XLRS.

Figure 1 shows example ERG waveforms obtained under the ERG_R (top), ERG_C (middle), and ERG_{R+C} (bottom) conditions for one control subject (53 years of age; thin traces) and Carrier 2 ($XLRS_C$; 50 years of age; thick traces). Data obtained with the 8 Hz stimulus are shown in the left column and data obtained with the 15 Hz stimulus are shown in the right column (note the difference in y-axis scale for the two columns).

ERG_R amplitude was small for both subjects at 8 Hz and the waveforms were similar in shape. The response amplitudes for the ERG_C obtained at 8 Hz were also similar for the carrier and control, but the shape of the response differed. That is, the control's response for each cycle was characterized by a small peak (indicated by the arrow) followed by a large peak, as reported previously [8]. The carrier's response was also characterized by two peaks, but the amplitude of the first peak was substantially larger, resulting in a waveform that was more bifurcated in shape than the control. A similar pattern was observed under the ERG_{R+C} condition (lower set of traces).

Responses obtained with the 15 Hz stimulus (right column) were more similar for the control and carrier in terms of amplitude, timing, and waveform shape compared to the 8 Hz responses. The carrier's ERG_C and ERG_{R+C} waveforms were somewhat more square-like in appearance, but otherwise generally similar. The amplitude for the ERG_R was small at 15 Hz (for both subjects), as expected given the generally sluggish response of the rod pathway. Also, the amplitude for the ERG_C and ERG_{R+C} was larger at 15 Hz compared to 8 Hz (for both subjects).

For each subject, the fundamental response amplitude and phase were derived by FFT for the 8 Hz stimulus and are plotted in Fig. 2 (left column). The range of normal amplitude (upper panel) for each condition is represented by the gray regions. Each symbol represents a different carrier, as given in Table 1. One control subject and Carrier 5 had ERG_{R+C} responses that did not exceed the noise level (SNR < 2.82); ERG_{R+C} data from these two subjects are not included in Fig. 2. The amplitude for the carriers was generally within the range of normal, with the exception of Carrier 1 who had a slightly larger than normal ERG_C amplitude (orange star) and Carrier 4 who had a

slightly larger than normal ERG_{R+C} amplitude (green square). The phase data obtained with the 8 Hz stimulus are shown in the lower panel. For the controls, there was a phase difference of approximately 180 deg between the ERG_R and ERG_C conditions and the phase of the control ERG_{R+C} was intermediate. These findings in the controls are consistent with previous reports [20,23,24]. There was substantial variation in the phase values of the carriers for all three conditions, ranging from normal to markedly advanced. The ERG_R phase was abnormally advanced in four of the six carriers (phase was advanced only slightly in two of these four carriers). The ERG_R phase of Carrier 4 (green square) was counter phase to the controls (approximately 180 deg phase advance). Inspection her waveforms indicated a high similarity in waveform shape and timing under the three paradigms. The ERG_C and ERG_{R+C} phase values were advanced, falling outside of the normal range in four (ERG_C) and three (ERG_{R+C}) of the six carriers. Only Carrier 3 (pink triangle) had normal phase values for all three conditions. The carriers' phase advances indicate a decrease in peak time, which is of note because most retinal changes (due to disease or aging, for example) typically act to slow the response (i.e. a phase delay).

The fundamental response amplitude and phase derived by FFT for the 15 Hz stimulus are plotted in the right column of Fig. 2. The amplitudes and phases were generally within the range of normal for all carriers. Two carriers (red circle and pink triangle; No. 2 and 3) had an ERG_R phase that was slightly delayed relative to normal, but the small amplitude ERG_R responses make the reliability of the subtle phase delays somewhat questionable, despite the statistically significant SNRs. Carrier 1 (orange star) had an ERG_{R+C} phase that was slightly delayed relative to normal. Similar to the

results for the 8 Hz stimulus, there was a phase difference of approximately 180 deg between the ERG_R and ERG_C conditions (for both the controls and carriers). The amplitude and phase of the ERG_{R+C} was similar to the ERG_C phase (for both groups), suggesting the responses for this condition were dominated by the cone pathway. These phase results are consistent with those reported previously in visually-normal subjects [20].

The second harmonic component of the responses was also derived by FFT and evaluated for the controls and carriers. Under the ERG_R condition, the second harmonic was not significantly different from noise for subjects in either group for both frequencies examined. Significant second harmonics were obtained for most subjects under the ERG_C and ERG_{R+C} conditions at both temporal frequencies. The carriers' amplitudes were within the normal range under all conditions for both frequencies. For the 8-Hz stimulus, 3 carriers (No. 4, 5, 6) had a phase advance under the ERG_C condition and two carriers (No. 3, 6) had a phase advance under the ERG_{R+C} condition. No second harmonic phase abnormalities were observed under the ERG_C and ERG_{R+C} conditions for the 15 Hz stimulus.

Discussion

This study evaluated rod-isolated, cone-isolated, and combined rod and cone ERGs as a possible means to identify electrophysiological abnormalities in carriers of XLRS. The results showed timing abnormalities in the 8 Hz flicker ERG in five of the six carriers. In contrast, the amplitudes of the carriers' 8 Hz flicker ERGs were generally within the range of normal, as were the amplitude and timing of the responses at 15 Hz. Thus, the abnormalities appear to be primarily restricted to phase advances for low

frequency flicker. Of note, the carriers' generally normal 15 Hz flicker ERGs suggest that potential differences between the carriers and controls (e.g. age, lens transmittance) did not meaningfully affect the results or our ability to isolate the rod and cone pathways. If systematic differences between the carriers and controls (unrelated to the *RS1* gene) were responsible for the phase abnormalities at 8 Hz, then similar phase abnormalities would also be expected at 15 Hz, which were not observed. The ISCEV standard ERGs were within the limits of normal for five of the six carriers. However, the nearly electronegative dark-adapted 3.0 cd s m^2 ERG of Carrier 1 is apparently an exception; to our knowledge, this is the first report of a full-field ERG abnormality in an XLRS carrier under ISCEV standard conditions.

The differences in the shape of the waveform for the carriers and controls (e.g. Fig. 1) may provide some insight into possible explanations for the carriers' 8 Hz phase advances. Fig. 1 shows that the 8 Hz ERG_C and ERG_{R+C} waveforms contained two peaks per cycle (for the control and carrier). This non-linearity in waveform shape was attributed previously to the response of the ON pathway to the increasing luminance of the sinusoidal stimulus (ON response; first peak) and to the response of the OFF pathway to the decreasing luminance of the sinusoidal stimulus (OFF response; second peak) [8]. The first peak is strongly attenuated in patients with XLRS [8], suggesting a loss of ON pathway function. In contrast to the results obtained in patients with XLRS, the carriers tended to have an abnormally large first peak. If, indeed, the first peak represents the ON response to the luminance increase, then the abnormally large first peak could be due to an abnormally large ON pathway response in the carriers.

Alternatively, the enhanced first peak could be related to an abnormally fast response, which seems more likely, given the phase advances shown in Fig. 2.

The effects of a fundamental phase advance, relative to normal, on the shape of the waveform can be appreciated in Fig. 3. The waveforms in the left column represent the mean 8 Hz ERG_C (top) and ERG_{R+C} (bottom) obtained from the controls (thin traces) and the carriers (thick traces). These waveforms are similar to those in Fig. 1, with the exception that the waveforms are derived from the subjects' mean data and only the fundamental and second harmonic components of the response are included, to simplify the modeling. The fundamental and second harmonic are sufficient to characterize the shape of the waveform. The ERG_C and ERG_{R+C} waveforms are characterized by two peaks (or a "shoulder" followed by a larger peak), with the second peak shifted leftward for the carriers (phase advance). The larger first peak (or enhanced shoulder) that is apparent in the mean carrier waveform relative to normal is also observed in the individual carrier's waveform shown in Fig. 1. The right column shows the effect of correcting the carriers' fundamental phase advances on the shape of the waveform. Specifically, the fundamental phase for the mean carrier waveform (thick traces in the left column) was set to that of the control mean and the waveform was re-generated (thick traces in the right column); the second harmonic was not altered in this model. It is clear that the fundamental phase correction results in the shape of the mean carrier waveform nearly matching that of the mean control waveform (thin trace; replotted from the left column). From this simulation we can conclude that the first peak (shoulder) seen in the carrier waveform is due to the fundamental phase advance of these subjects

and that correcting the phase advance nearly equates the carrier and control waveforms.

As noted in the Introduction, the ERG_{R+C} condition was of particular interest as it allows insight into rod-cone interactions in the flicker ERG. That is, the ERG_{R+C} is generated by the combined activity of the rod and cone pathways, which are modulated in phase at the same contrast. Previous work has shown that the amplitude of the ERG_{R+C} can be predicted by vector summation of the ERG_R and ERG_C responses [20,23,24,26]. Furthermore, under the conditions used in the present study, the amplitude of the ERG_{R+C} is attenuated due to destructive interference between the ERG_R and ERG_C responses, which have opposite phase. This can be seen in both the carrier and control data of Fig. 2, in which the ERG_{R+C} amplitude is less than the ERG_C amplitude. A particularly clear example of this interaction is apparent in data of the Carrier 5 (Fig. 2, black diamonds) who had nearly equal amplitude ERG_R and ERG_C responses that were approximately counter phase; for this carrier, the ERG_{R+C} was extinguished.

If there were abnormal rod-cone interactions in the carriers' 8 Hz flicker ERG (for example, due to a timing change in the rod or cone response), then destructive interference between the rod and cone pathways would be reduced (or absent) and the ERG_{R+C} amplitude would be larger than the ERG_R and ERG_C amplitudes. This was generally not observed, with the exception of Carrier 4 who had similar ERG_R and ERG_C phases, resulting in summation of these responses and an abnormally large ERG_{R+C} amplitude (Fig. 2; green squares). The type of rod-cone interaction examined herein (vectorally summed ERG_R and ERG_C responses) is likely different from the rod-cone

interaction in carriers of XLRS reported psychophysically [16,27]. Specifically, the rod-cone interaction measured psychophysically may be due to a suppressive effect of rods on nearby cones, a spatially localized effect not found for large (ganzfeld) stimuli [27,28]. Thus, the abnormal rod-cone interaction that we observed in one carrier (Fig. 2; green squares) is not necessarily related directly to the abnormal rod-cone interaction measured psychophysically.

In summary, abnormalities in the timing of the 8 Hz flicker ERG can occur in carriers of XLRS. Based only on the 8 Hz flicker ERG phase, we were able to identify an abnormality in five of six carriers that ranged from subtle to marked. The phase abnormalities appear to demonstrate an effect of Lyonization on retinal function in carriers of XLRS. The magnitude of the phase abnormality differed among the carriers, which may be attributable to the extent of abnormal X-chromosome expression. Thus, the 8-Hz flicker ERG recorded under rod-, cone-, and combined rod and cone conditions may be useful for detecting and studying retinal function in XLRS carriers.

Funding: The National Institutes of Health, Research to Prevent Blindness, the Pangere Family Foundation, and the Grousbeck Family Foundation provided financial support in the form of funding. The sponsors had no role in the design or conduct of this research.

Conflict of Interest: All authors certify that they have no affiliations with or involvement in any organization or entity with any financial interest (such as honoraria; educational grants; participation in speakers' bureaus; membership, employment, consultancies, stock ownership, or other equity interest; and expert testimony or patent-licensing arrangements), or non-financial interest (such as personal or professional relationships, affiliations, knowledge or beliefs) in the subject matter or materials discussed in this manuscript.

Ethical approval: All procedures performed in studies involving human participants were in accordance with the ethical standards of the institutional and/or national research committee and with the 1964 Helsinki declaration and its later amendments or comparable ethical standards.

Informed consent: Informed consent was obtained from all individual participants included in the study.

References

1. Sauer CG, Gehrig A, Warneke-Wittstock R, Marquardt A, Ewing CC, Gibson A, Lorenz B, Jurklies B, Weber BH (1997) Positional cloning of the gene associated with x-linked juvenile retinoschisis. Nat Genet 17(2):p.164-170.
2. Wang T, Zhou A, Waters CT, O'Connor E, Read RJ, Trump D (2006) Molecular pathology of x linked retinoschisis: Mutations interfere with retinoschisin secretion and oligomerisation. Br J Ophthalmol 90(1):p.81-86.
3. Deutman AF (1971) The hereditary dystrophies of the posterior pole of the eye. Van Gorcum, Assen,
4. George ND, Yates JR, Moore AT (1995) X linked retinoschisis. Br J Ophthalmol 79(7):p.697-702.
5. Roesch MT, Ewing CC, Gibson AE, Weber BH (1998) The natural history of x-linked retinoschisis. Can J Ophthalmol 33(3):p.149-158.
6. Sieving PA, MacDonald IM, Chan S (1993) X-linked juvenile retinoschisis. In: Pagon RA, Adam MP, Ardinger HH et al. (eds) Genereviews(r). Seattle (WA),
7. Peachey NS, Fishman GA, Derlacki DJ, Brigell MG (1987) Psychophysical and electroretinographic findings in x-linked juvenile retinoschisis. Arch Ophthalmol 105(4):p.513-516.
8. Alexander KR, Fishman GA, Grover S (2000) Temporal frequency deficits in the electroretinogram of the cone system in x-linked retinoschisis. Vision Res 40(20):p.2861-2868.
9. Kellner U, Brummer S, Foerster MH, Wessing A (1990) X-linked congenital retinoschisis. Graefes Arch Clin Exp Ophthalmol 228(5):p.432-437.

10. Kellner U, Foerster MH (1993) Cone dystrophies with negative photopic electroretinogram. Br J Ophthalmol 77(7):p.404-409.

11. Falsini B, Iarossi G, Porciatti V, Merendino E, Fadda A, Cermola S, Buzzonetti L (1994) Postreceptoral contribution to macular dysfunction in retinitis pigmentosa. Invest Ophthalmol Vis Sci 35(13):p.4282-4290.

12. Alexander KR, Barnes CS, Fishman GA (2001) Origin of deficits in the flicker electroretinogram of the cone system in x-linked retinoschisis as derived from response nonlinearities. J Opt Soc Am A Opt Image Sci Vis 18(4):p.747-754.

13. Murayama K, Kuo CY, Sieving PA (1991) Abnormal threshold erg response in x-linked juvenile retinoschisis - evidence for a proximal retinal origin of the human str. Clinical Vision Sciences 6(4):p.317-322.

14. Wu G, Cotlier E, Brodie S (1985) A carrier state of x-linked juvenile retinoschisis. Ophthalmic Paediatr Genet 5(1-2):p.13-17.

15. Kim LS, Seiple W, Fishman GA, Szlyk JP (2007) Multifocal erg findings in carriers of x-linked retinoschisis. Doc Ophthalmol 114(1):p.21-26.

16. Arden GB, Gorin MB, Polkinghorne PJ, Jay M, Bird AC (1988) Detection of the carrier state of x-linked retinoschisis. Am J Ophthalmol 105(6):p.590-595.

17. Jay B (1985) X-linked retinal disorders and the lyon hypothesis. Trans Ophthalmol Soc U K 104 (Pt 8):p.836-844.

18. Krill AE (1969) X-chromosomal-linked diseases affecting the eye: Status of the heterozygote female. Trans Am Ophthalmol Soc 67:p.535-608.

19. Lyon MF (1962) Sex chromatin and gene action in the mammalian x-chromosome. Am J Hum Genet 14:p.135-148.

20. McAnany JJ, Park JC, Cao D (2015) Rod- and cone-isolated flicker electroretinograms and their response summation characteristics. Vis Neurosci 32:p.E018.

21. McCulloch DL, Marmor MF, Brigell MG, Hamilton R, Holder GE, Tzekov R, Bach M (2015) Iscev standard for full-field clinical electroretinography (2015 update). Doc Ophthalmol 130(1):p.1-12.

22. McAnany JJ, Nolan PR (2014) Changes in the harmonic components of the flicker electroretinogram during light adaptation. Doc Ophthalmol 129(1):p.1-8.

23. Park JC, Cao D, Collison FT, Fishman GA, McAnany JJ (2015) Rod and cone contributions to the dark-adapted 15-hz flicker electroretinogram. Doc Ophthalmol 130(2):p.111-119.

24. Cao D, Pokorny J, Grassi MA (2011) Isolated mesopic rod and cone electroretinograms realized with a four-primary method. Doc Ophthalmol 123(1):p.29-41.

25. Meigen T, Bach M (1999) On the statistical significance of electrophysiological steady-state responses. Doc Ophthalmol 98(3):p.207-232.

26. Kremers J, Scholl HP (2001) Rod-/l-cone and rod-/m-cone interactions in electroretinograms at different temporal frequencies. Vis Neurosci 18(3):p.339-351.

27. Arden GB, Hogg CR (1985) Rod-cone interactions and analysis of retinal disease. Br J Ophthalmol 69(6):p.404-415.

28. Arden GB, Frumkes TE (1986) Stimulation of rods can increase cone flicker ergs in man. Vision Res 26(5):p.711-721.

Figure captions

Figure 1: ERG_R waveforms (top pairs of traces; blue), ERG_C waveforms (middle pairs of traces; red), and ERG_{R+C} waveforms (bottom pairs of traces; black) are shown. The thin and thick waveforms represent the responses of a representative control and a XLRS carrier, respectively (also indicated to the right). The left column shows the traces obtained with the 8 Hz stimulus and the right column shows the traces obtained with the 15 Hz stimulus. For clarity, only four cycles of the waveforms are shown and frequencies above 60 Hz were removed by low-pass filtering to minimize the high-frequency noise. The peak times of the control waveforms are marked by the vertical dashed lines. The arrows highlight waveform features discussed in the text.

Figure 2: Fundamental amplitude (top) and phase (bottom) for the 8 Hz (left column) and 15 Hz (right column) stimuli. Data are shown for the ERG_R paradigm (first data set), ERG_C paradigm (second data set), and ERG_{R+C} paradigm (third data set). The normal control range for each paradigm is indicated by the gray bars and the mean control response is indicated by the horizontal black line. Each symbol represents a different XLRS carrier, as given in Table 1.

Figure 3: Effect of correcting the XLRS carriers' fundamental phase advances on waveform shape. The left column shows the mean waveforms obtained under the ERG_C (top pair of traces; red) and ERG_{R+C} (bottom pair of traces; black) paradigms. The control (thin traces) and carrier (thick traces) are superimposed. The right column shows the mean waveforms for the carriers after correcting their fundamental phase advance (thick traces). The control waveforms (thin traces) are

replotted from the left column for comparison.

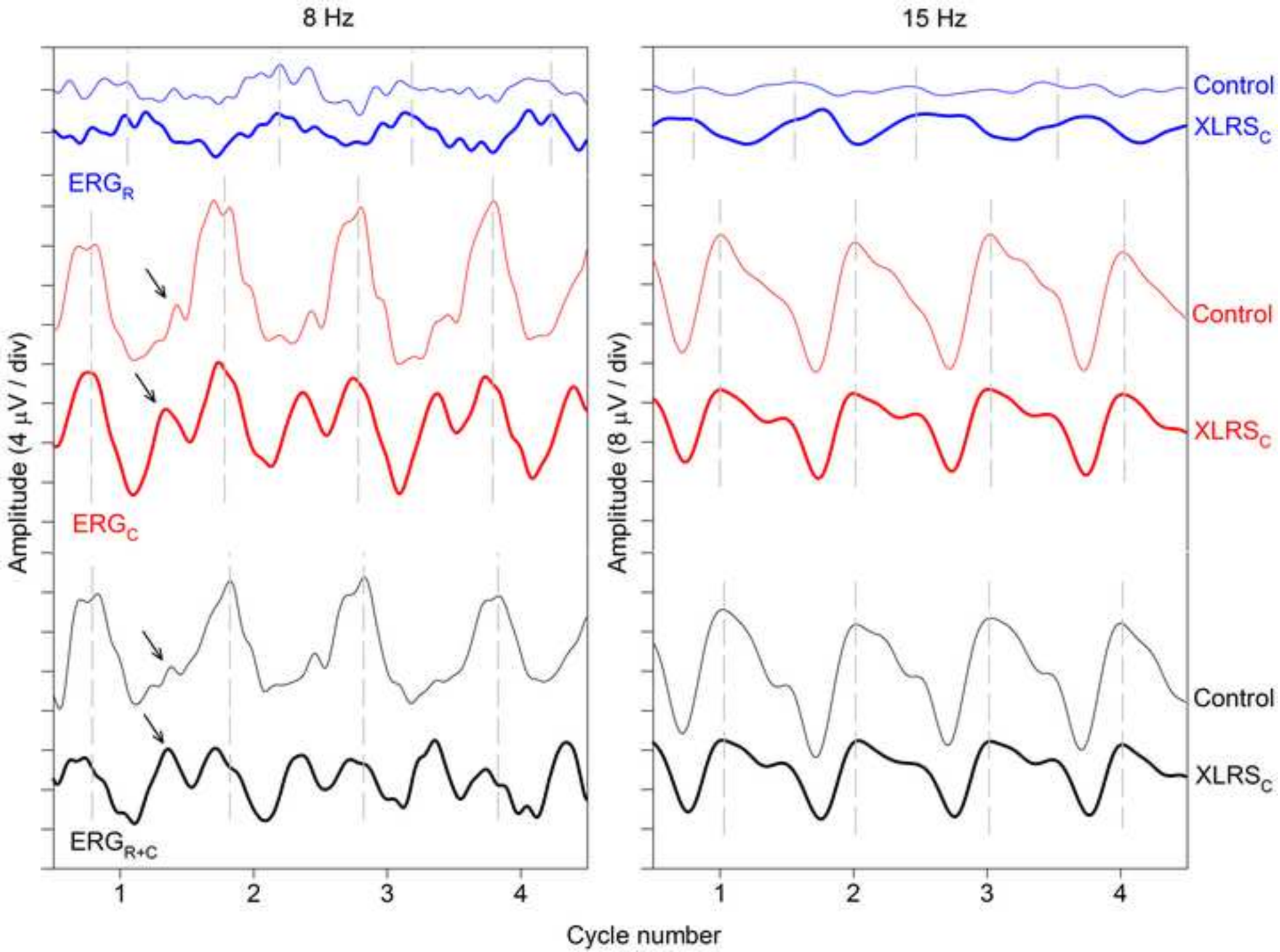
8 Hz
15 Hz
ERG$_R$
ERG$_C$
ERG$_{R+C}$
Control
XLRS$_C$
Control
XLRS$_C$
Control
XLRS$_C$
Amplitude (4 μV / div)
Amplitude (8 μV / div)
1
2
3
4
Cycle number

Figure 2

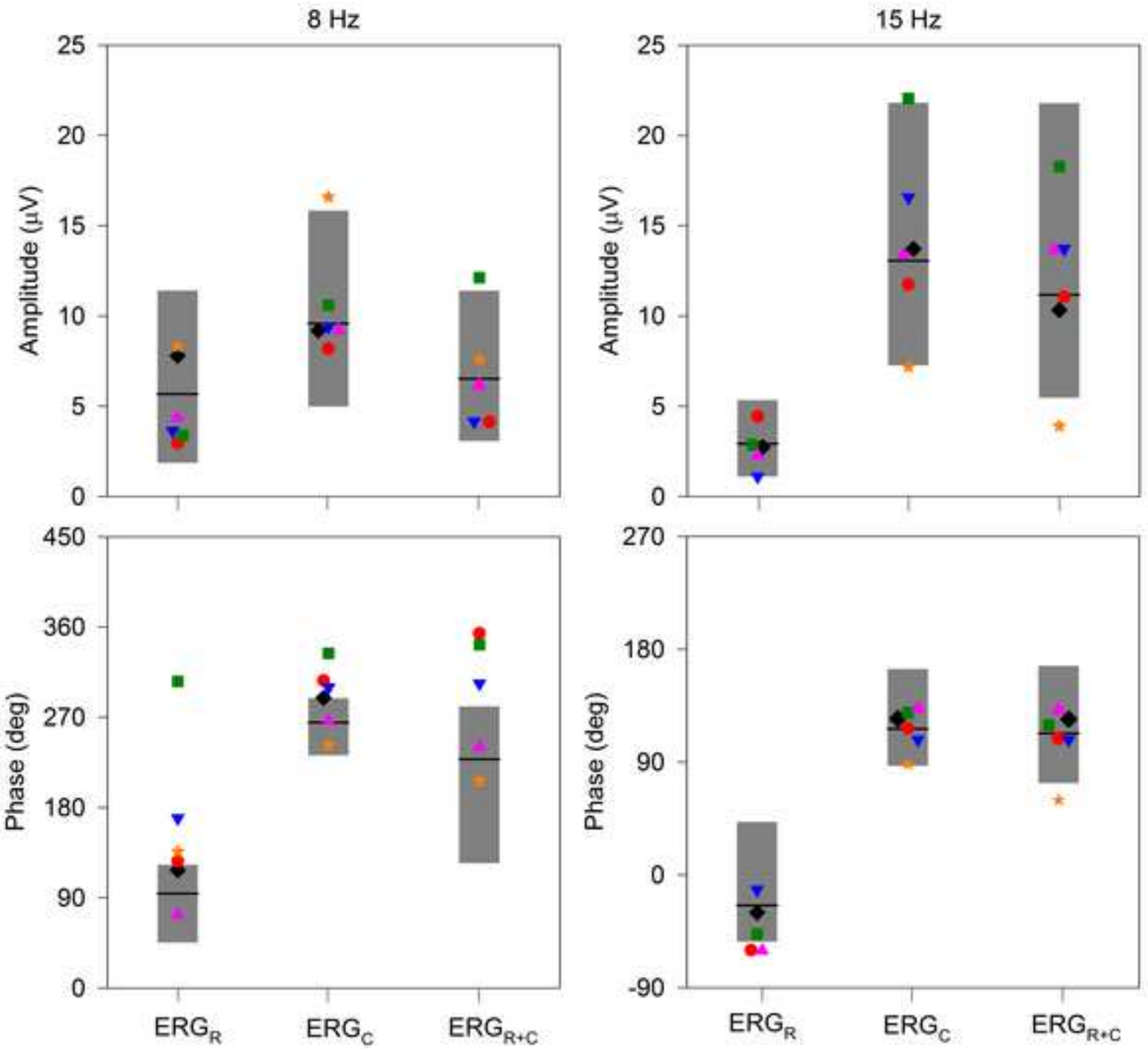
8 Hz
15 Hz
Amplitude (μV)
Phase (deg)
25
20
15
10
5
0
450
360
270
180
90
0
-90
ERG$_R$
ERG$_C$
ERG$_{R+C}$

Figure 3

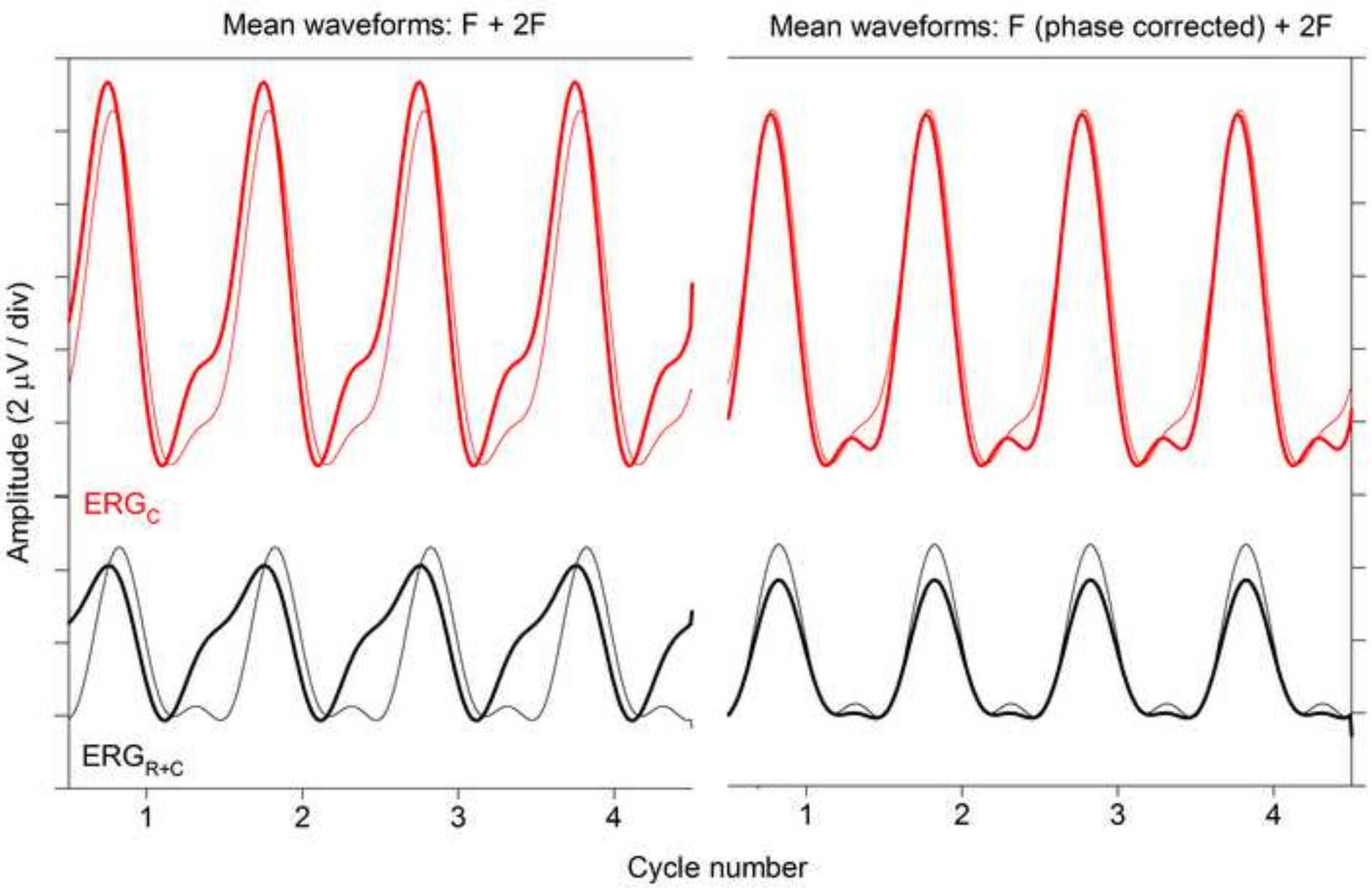
Mean waveforms: F + 2F
Mean waveforms: F (phase corrected) + 2F
Amplitude (2 μV / div)
ERG$_C$
ERG$_{R+C}$
1
2
3
4
1
2
3
4
Cycle number

Table 1: Subject characteristics

Carrier No.	Symbol	Age	*RS1* Mutation
1		34	Not available
2		50	IVS4-10del7gTTCTCGGins1gC (c.327-10delTTCTCGGinsC)
3		52	Pro193Leu CCC>CTC (c.578C>T)
4		57	Arg141His CGC>CAC (c.422G>A)
5		61	Gly74del17gGGGAGGTCACACCGGACins20TCCCCTGACCGGGTTAGAGT (c.221_237delGGGAGGTCACACCGGACinsTCCCCTGACCGGGTTAGAGT)
6		66	Gly70Ser GGT>AGT (c.208G>A)
Control range		27 to 59	

Table 2: LED parameters

			Rod+cone modulation		Rod-isolating stimulus		Cone-isolating stimulus	
LED peak λ (nm)	Luminance (scot. cd/m^2)	Luminance (phot. cd/m^2)	Contrast	Phase	Contrast	Phase	Contrast	Phase
465	2.83	0.35	0.40	0	0.31	180	0.71	0
515	15.93	5.41	0.40	0	0.80	0	0.40	180
593	4.79	19.01	0.40	0	0.53	180	0.93	0
642	0.37	8.23	0.40	0	0.72	0	0.32	180

Table 3: ISCEV standard ERG results

Carrier No.	DA 0.01		DA 3.0					LA 3.0				LA 3.0 flicker	
	b-wave amp	b-wave IT	a-wave amp	a-wave IT	b-wave amp	b-wave IT	b/a ratio	a-wave amp	a-wave IT	b-wave amp	b-wave IT	Peak-trough amp	Peak IT
1	130	94	124*	14	139*	48	1.1*	29	13	90	30	47	26
2	297	89	227	14	529	47	2.3	45	13	235	29	51	24
3	268	91	219	14	475	48	2.2	36	14	141	30	45	25
4	220	94	240	14	450	50	1.9	40	14	143	29	48	24
5	268	93	223	15	437	46	2.0	33	13	135	28	41	25
6	143	94	164	14	310	47	1.9	32	14	148	29	45	26
Control range	106 to 401	79 to 99	144 to 432	14 to 15	216 to 712	45 to 50	1.4 to 3.6	28 to 56	12 to 14	86 to 237	27 to 31	22 to 88	24 to 27

DA, dark adapted; LA, light adapted; amp, amplitude (μV); IT, implicit time (ms); the asterisk indicates responses that are outside of the control range.